Residual stresses in injection molded products

ARTICLE *in* JOURNAL OF MATERIALS SCIENCE · JULY 2014

Impact Factor: 2.37 · DOI: 10.1007/s10853-014-8170-y

2 AUTHORS:


A. Guevara-Morales
Tecnológico de Monterrey


U. Figueroa-López
Tecnológico de Monterrey

J Mater Sci (2014) 49:4399–4415
DOI 10.1007/s10853-014-8170-y

REVIEW

Residual stresses in injection molded products

A. Guevara-Morales · U. Figueroa-López

Received: 12 December 2013 / Accepted: 13 March 2014 / Published online: 28 March 2014

Abstract Injection molding is the most widely used processing technique for polymers. It offers several advantages over other processing conditions such as good surface finish, the ability to process complex parts without the need of secondary operations, and low cost for mass production. However, because of the complex deformation, and thermal and pressure histories that the polymer melt experiences during processing, residual stresses develop. These stresses act internally at room temperature and have the same effects on the material as externally applied stresses do, resulting in shrinkage and warpage of the product. In recent years, with the development and use of engineering plastics in an increasing number of applications, and with the tougher quality control policies in industries such as the automotive, the effects of residual stresses in product quality and performance have raised great interest. This review reports up-to-date advances in the field of residual stresses developments in polymers, with special attention given to injection molded products. Flow- and thermal-induced residual stresses are reported. Emphasis is given to the processing parameters that most influence residual stresses during injection molding as well as the effect of residual stresses not only on warpage but also on other material properties.

A. Guevara-Morales (✉) · U. Figueroa-López
Department of Mechatronics Engineering, ITESM-CEM, 52926 Atizapán de Zaragoza, Estado de México, Mexico
e-mail: a.guevaram@itesm.mx

U. Figueroa-López
e-mail: ufiguero@itesm.mx

Introduction

Injection molding is the most widely used processing technology for plastics. It is an extremely versatile and flexible process for producing a wide range of simple or complex plastic components with high precision, good surface finish, and low operational costs for mass production. It consists of three stages: filling, packing, and cooling. First, raw material is heated until a homogeneous melt is obtained, which is then forced by pressure into a cavity. When filling is nearly completed, a packing pressure is applied to fill the remaining volume of the cavity and to compensate for the shrinkage caused by cooling of the material. When the gate of the cavity solidifies, no more pressure is needed and the material is allowed to cool into the desired shape. Once the part is rigid enough, the mold is opened and the part is ejected, at which time the cycle is repeated.

During these processes, the polymer melt experiences a complex deformation, and temperature and pressure histories that affect the final properties of the component. Residual stresses are originated due to the high pressure, temperature differences, and relaxation of polymer chains, which result in shrinkage and warpage of the product.

Engineering plastics are a group of thermoplastic materials that exhibit superior mechanical and thermal properties as compared to the more widely used commodity plastics. They are used in applications generally requiring exceptional properties such as stiffness, toughness, and heat and chemical resistance. To meet the technical requirements in demanding applications such as the automotive industry, different additives, fillers, and modifiers are commonly used. However, these additives also affect the behavior of the polymer melt. Opposite to commodity plastics that are relatively easy to process, engineering plastics processing is more complex, requiring higher temperatures and pressures, having a significant effect on residual stresses.

Current demands on close dimensional tolerances and high dimensional stability make it necessary to be able to predict residual stresses and warpage of the molded part. This requires a deep understanding of the mechanisms that originate residual stresses and the factors that influence them. Residual stresses have been a topic of interest in the last decades. Several reviews on the build-up of flow-induced stresses during injection molding are found in the literature [1–6]. However, most of these reviews are from three decades ago, and therefore, an update to more recent work is required.

The aim of this review is to describe the up-to-date state of knowledge regarding residual stresses in injection molded products, including not only the description of its formation mechanisms and models but also a review of the processing conditions that most affect them. The effect of residual stresses in different material properties which affect the product performance is also included, as well as a summary of the different residual stress measurement techniques. At the end, some comments on the current state of the art are included.

Types of residual stresses in injection molding products

Residual stresses mainly originate from two effects [7, 8]: the flow-induced stresses, which correspond with the orientation of the molecules and are developed during the filling and packing of the polymer into the cavity; and the thermall-induced stresses developed during the cooling stage. Generally, flow-induced stresses are an order of magnitude smaller than the thermal-induced stresses and are usually neglected [6, 7]. However, some authors [9] suggest that it is impossible to neglect them as they induce anisotropy of several properties [7, 10] because of the different frozen-in orientations of polymer molecules, which affect the long-term dimensional stability of the component. In the following sections, these two types of stresses, their main features, and build-up mechanisms and models will be described.

Flow-induced stresses

During the injection molding process, orientation [11, 12] and flow-induced stresses develop during the viscoelastic flow of the polymer in both the filling and the post-filling stage [9, 13, 14]. In the 1980s, attention was focused on the filling stage [6, 15]; however, calculation of the flow-induced stresses in the filling stage has been extended to the post-filling stage [16–18] because birefringence measurements [19–21] have shown that during packing, large orientations are also developed [22]. They develop when the polymer is in its fluid or melt state and are accompanied with alignment of the chain molecules with respect to the flow direction [23]. Because of the high solidification rates in injection molding, the complete relaxation of this flow-induced stresses is prevented and they remain locked within the solidified material as reported by Bushko and Stokes [24–27]. Analytical investigations of flow-induced stresses require an accurate calculation of the moving flow front during filling and the chain relaxation in the post-filling stage. Since rheological and geometrical nonlinearities are involved in polymer melt flow [28–31], the task becomes difficult and extremely complex, thus many times simple one-dimensional theories are used, which allow to grasp the main features of the flow.

Flow-induced stresses formation mechanism

Daly et al. [5] described the build-up or formation mechanism of flow-induced stresses during filling and packing based on Vinogradov [32] earlier qualitative study. It is suggested that during filling, polymer chains are stretched and oriented in the flow direction (Fig. 1a). During cooling, these deformations relax. The more oriented the chains, the more the relaxation they will undergo. However, relaxation of the most oriented chains (in the outer layers) is restricted by the less oriented inner layers (Fig. 1b), and thus flow-induced residual stress in the filling stage is tensile in the outer layers and compressive in the inner ones.

For the packing stage, three cases are presented and they are illustrated in Fig. 2. In the first case, Fig. 2a, it is assumed that the polymer melt is not sufficiently compressed and that during the cooling stage, the pressure in the core layers fall to zero when the thickness of the solidified outer layer is relatively small. Upon further cooling, the inner layers reduce their volume and compress the outer layers, yielding a compressive-skin–tensile-core distribution, usually evident as a sink mark. This profile is always observed in free quenched products [33]. Similar results were found by Sandilands and White [34] and Mlekusch [35]. For the case when the melt is over-compressed, Fig. 2b, the pressure at the inner cores remains very high even after complete cooling, and therefore, the stress distribution will be tensile-skin–compressive core, as found by Wang and Young [36]. In the third case, Fig. 2c, it is assumed that the pressure in the core layers fall to zero when the thickness of the solidified outer layer is much greater than that of the inner ones, resulting in a more complex distribution: tensile-skin—compressive-subskin—tensile core, as reported by Young [8] and Zoetelief et al. [7].

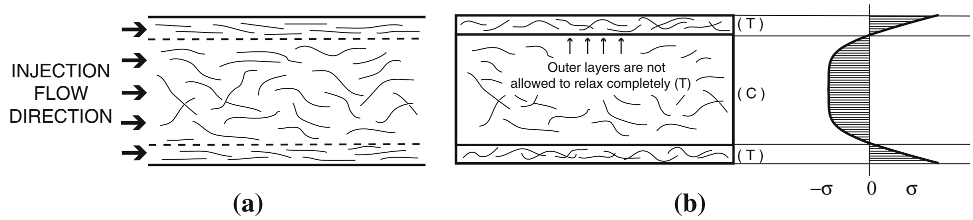

Fig. 1 Flow-induced stresses during the filling stage: **a** stretched polymer chains and **b** relaxed polymer chains

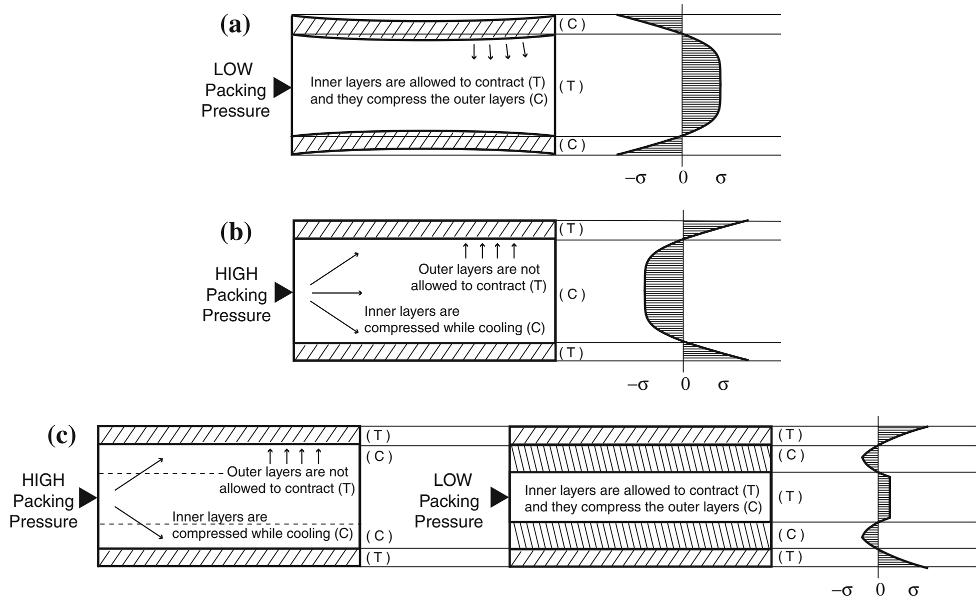

Fig. 2 Flow-induced stresses during the packing stage subjected to **a** low packing pressure (under-compression), **b** high packing pressure (over-compression), and **c** high/low packing pressure profile

Jansen et al. [37] found a similar behavior when molding plates at different packing pressures. They reported that as the packing pressure was increased, the plate started warping toward the opposite direction. This is, at low packing pressures it warped toward the hot side, as the pressure was increased, warpage was reduced, but as the packing pressure continued to increase, warpage increased toward the cold side. As residual stresses originate warpage, this change in warpage behavior must be related to a change in the residual stress distribution. Since the pressure is not uniform along the flow path during injection molding (it is higher at the gate and it decreases along the flow path), all three cases can be present in a single component, resulting in different residual stress distributions. Therefore, it is important to be able to predict or monitor the temperature and pressure history during the complete injection molding cycle, which are known as temperature and pressure profiles.

Flow-induced stresses models

The three-dimensional governing equations of the non-isothermal flow of viscoelastic fluids are [6]

(1) Continuity equation:
$\frac{\dot{\varrho}}{\varrho} + \vec{\nabla} \cdot \vec{v} = 0$, where ϱ represents the density, and $\vec{\nabla} \cdot \vec{v}$ is the divergence of the velocity field.

(2) Momentum equation:
$\vec{\nabla} \cdot \sigma + \varrho \vec{f} = \varrho \dot{\vec{v}}$, where σ is the Cauchy stress tensor and $\vec{f}$ is the body force per unit mass.

(3) Energy equation:
$\varrho \dot{\varepsilon} = \sigma : D - \vec{\nabla} \cdot \vec{h} + \varrho r$, where ε is the specific internal energy, D is the rate of strain tensor, $\vec{h}$ the heat flux, and r is an internal heat source.

To solve these governing equations, constitutive equations for ϱ, σ, ε, $\vec{h}$, and r must be given.

During the last decades, different approaches to the problem have been developed. Table 1 summarizes some of the most important studies developed in this area. It is observed that a great amount of this work has been based on Leonov viscoelastic constitutive equation [38], where irreversible thermodynamics are used for constructing the rheological equations capable of describing the behavior of polymer melts in a range of large elastic strains. It is also observed that, depending on the processing conditions, reported values of residual stresses are approximately up to

Table 1 Flow-induced stresses models and simulations

Authors	Approach	Results
Based on Leonov model [38]		
Isayev and Hieber [40]	One-dimensional, unsteady non-isothermal flow of polymer between two parallel plates	Stresses increase in magnitude moving inwards from the wall. Maximum stress ≈ 2.0 MPa
	Non-isothermal relaxation following cessation of flow	
Mavridis et al. [41]	FEM solution of the fountain flow problem, analyzing its effect on the deformation in the fluid during filling	Frozen-in stresses were calculated and maximum values of birefringence distributions agreed with published experimental results
Baaijens [6]	Viscoelastic material behavior (direct approach)	Calculated both flow and thermal-induced stresses
	Generalized Newtonian material behavior (indirect approach)	Mold elasticity has an important effect on the pressure history
		TCT distribution for PC ≈ 8.0/−8.0/2.0 MPa
Flaman [42, 43]	Numerical simulation of the build-up and relaxation of molecular orientation	Prescription of a specified packing pressure profile can reduce the frozen-in birefringence
	Volumetric responses were predicted using the Tait equation and a second equation developed by Spencer and Gilmore [44]	
	A WLF equation was used for the temperature and pressure dependence	
Kabanemi et al. [39]	Flow and thermoviscoelastic stresses during injection molding based on Baaijens indirect approach: kinematics were calculated from a generalized Newtonian model and flow stresses were updated using a Wagner model	Flow-induced stresses results virtually coincide which those of Baaijens [6], although the effect of compressibility and the influence of the packing stage were neglected
		Maximum stress in PS ≈ 0.5 MPa
Other analytical and semi-analytical models		
Greener et al. [45]	Analytical model for the flow, heat transfer and relaxation in centered-gated cavities	A good agreement between experimental data and birefringence predictions was found
	Evolution of stress was calculated with the nonlinear viscoelastic model of Wagner [46] and the work by Matsui and Bogue [47]	A good prediction of the effects of melt and mold temperature, and injection speed on residual stresses was found
		Stresses increase in magnitude moving inwards from the wall. Maximum stress in PC ≈ 0.5 MPa, for PS ≈ 1 MPa
Cao et al. [23]	Semi-analytical method to simulate the flow-induced stresses developed during the filling and packing stage	Melt temperature strongly determine the flow-induced stresses
	Hele–Shaw flow [13] was assumed, and the Phan–Thien–Tanner [48] model was employed to describe the viscoelastic behavior of the melt	Experimental results agreed well with numerical results
	Pressure was determined with the conventional Galerkin method [49]	Stresses increase in magnitude moving inwards from the wall. Maximum stress in PS ≈ 0.5 to 5 MPa depending on processing conditions
Zhou et al. [50]	Simulated the history and distribution of residual stresses in simple plate specimens using the same material model as that of Zoetelief et al. [7]	*TCT* distribution for ABS ≈ 3.0/−6.0/3.0 MPa
	Packing and cooling stages were considered so that pressure, temperature and relaxation effects were taken into account	

TCT tensile-skin/compressive-subskin/tensile-core distribution (Fig. 2c), *CT* compressive-skin/tensile-core distribution (Fig. 2a)

8 MPa, both in tension and compression when the packing stage is considered. However, when packing is neglected (i.e., Kabanemi et al. [39]) reported values are much lower.

It has been noticed that most of the research work on residual stresses and warpage has been focused on amorphous polymers. However, it is clear from several studies [51–55] that the flow and thermal history experienced by the melt during injection can enhance crystallization kinetics, and thus lead to different types of crystalline structures, which is known as flow-induced crystallization. This is of great technological importance as polymer properties are to a great extent affected by morphology [56–61]. Differences in crystallinity and orientation throughout an injected product will lead to anisotropy and other changes in mechanical properties as reported by Santis et al. [62] and Pantani et al. [63]. The crystalline phase has a tighter packing than the amorphous phase and, therefore, a higher density. This densification process is accompanied by changes in mechanical properties such as elastic modulus, yield strength, elongation at break, ultimate strength, and thermal properties such as the thermal expansion coefficient. This, in turn, will have an effect on residual stress distributions. Various models [64–69] have been developed to describe the crystallization process of polymers. However, most of these studies are limited to idealized situations, in which external conditions such as temperature or cooling rate are considered as constant. In real situations, however, the polymer is cooled down at different rates and with high thermal gradients, which makes the crystallization process dependent on instantaneous conditions [70]. Several modifications of the Avrami theory [65, 71, 72] have been proposed over the years to model non-isothermal crystallization. Most of these models neglect spherulite impingement and variations in cooling rates. Empirical or experimental approaches have also been developed to calculate the main parameters of non-isothermal crystallization [73] in which crystallization kinetics are observed by differential scanning calorimetry.

For the particular case of injection molding, an exhaustive literature review of the modeling of morphology evolution during processing of semicrystalline polymers was presented by Pantani et al. [74], including a thorough analysis of the effect of different processing parameters in the morphology of the product. However, work investigating the effect of crystallinity distribution on residual stresses in plastic parts is still required.

Thermally induced stresses

Thermoplastics processing usually involves the non-uniform cooling of molten polymer, which results in the presence of thermal residual stresses in the final product. The thermoviscoelastic theory of residual stresses was initially developed for inorganic glasses [75–79], with previous work by Adams and Williamson [80] on the annealing of glass, and first applied to polymers by Struik [81] under free or unconstrained quenching conditions.

According to his work, it can be assumed that during injection molding, the outer layer of the polymer melt, in contact with the cold mold, undergoes an instantaneous step change in temperature, while the core remains hot. Heat removal is almost entirely from the outer surfaces where a solid external layer is formed. At this point, the surface layers are almost stress free as they were allowed to contract freely. The inner layers are still hot and behave as a liquid free of stresses. While cooling continues, the solidifying material further in is prevented from freely contracting by the outer solid layer. A compressive-skin/tensile-core distribution as the one shown in Fig. 2a is obtained.

These results were reported by Siegmann et al. [2], who investigated the distribution of residual stresses in quenched PPO. Compressive stresses were measured at the surface layers, while tensile stresses were measured in the inner layers. The level of residual surface stresses was found to depend on both the total temperature difference during cooling and the initial specimen temperature. Similarly, Rigdahl [82] used the finite element method to calculate the distribution of residual internal stresses in an injection molded PS specimen. By determining the temperature distributions in the plate and its variation with cooling time, the corresponding stress distribution was found. It was found that the surface layer of the plate is subject to compressive stresses, while the interior accommodates stresses of tensile type. Anisotropy and viscoelastic relaxation have been neglected as well as the effect of packing pressure.

However, during injection molding, the polymer melt conditions differ from those of free quenching. The material is constrained by the mold geometry, the holding pressure, and the adhesion between the mold and part, which change the thermal-induced residual stresses buildup. Therefore, shrinkage of the solidified layer is prevented, and a residual stress distribution as the one shown in Fig. 2c is obtained.

Thermally induced stresses formation mechanism

Zoetelief et al. [7] illustrated the development of residual thermal stresses using the schematic representation similar as the one shown in Fig. 3. This representation is analogous to the work presented by Struik [81] in which the theory of the quenching of flat glass plates is described and shown to be applicable to polymers. Similar numerical formulations were used by Jansen and Titomanlio [83]. As shown in Fig. 3, cooling is idealized in five steps and pressure varies as a function of time. T_{freeze} is the glass transition temperature and it is assumed that the material behaves as an ideal fluid when $T > T_{\text{freeze}}$, and as a linear elastic material when $T < T_{\text{freeze}}$. Temperature drops and residual stresses develop as follows:

$t = t_0$: Homogeneous temperature throughout the specimen; pressure = 0; material free of stresses.

$t = t_1$: No-slip condition hinders contraction of outer layers; small tensile stress develops (Fig. 3a).

$t = t_2$: Holding pressure $\sigma = -p_{\text{h}}$ acts on the melt; the rigid shell is also compressed; stress levels decrease by $\Delta\sigma = \nu p_{\text{h}}/(1-\nu)$, where ν is the Poisson's ratio (Fig. 3b).

$t = t_3$: Packing stage: pressure remains constant; a small layer solidifies, and its contraction is hindered, decreasing compressive stresses in it (Fig. 3c).

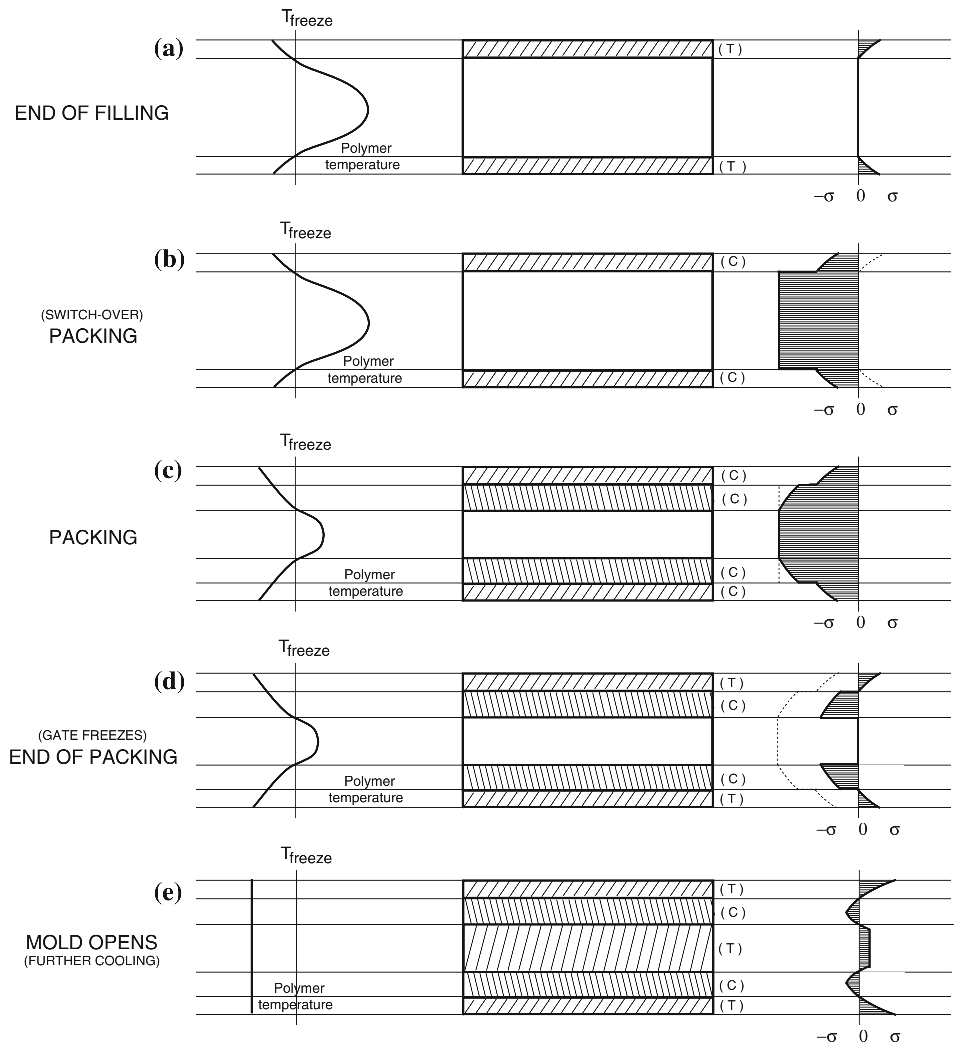

Fig. 3 Thermally induced residual stress development in injection molded products: **a** t_1, **b** t_2, **c** t_3, **d** t_4, and **e** t_5. Drawn based on [7]

$t = t_4$: Packing stage finishes, pressure is set to zero; stress in the melt disappears, and the stress levels increase by $\Delta\sigma$ (Fig. 3d).

$t = t_5$: Mold is opened, product is released from the mold; further cooling sets tensile stresses in the core, which are in equilibrium with the rest of the specimen. At the end of this interval, a tensile-skin, compressive-subskin, and tensile-core distribution are obtained, which have been reported by several authors [33, 35, 84–86] (Fig. 3e).

Thermally induced stresses models

Initially, most of the models developed to predict residual stresses or warpage of plastic parts assumed a linear thermoelastic behavior in which the conservations of momentum and energy equations are similar to those presented in "Flow-induced stresses models" Section with the Cauchy stress tensor, commonly decomposed into a hydrostatic part p, and a deviatoric part σ^{d} is determined by [5]

$$\sigma = pI + \sigma^{\mathrm{d}},$$

where I is the identity tensor,

$$p = \int_0^t \left[\frac{\alpha}{\kappa}T - \frac{i}{\kappa}\mathrm{tr}D\right]\mathrm{d}s,$$

$$\sigma^{\mathrm{d}} = 2\int_0^t G(\xi(t),\xi(s))D(s)\mathrm{d}s, \quad \text{and}$$

$$\xi(t) = \int_0^t \frac{1}{a_{\mathrm{T}}}\mathrm{d}s,$$

where α is the coefficient of thermal expansion, κ the coefficient of compressibility, $G(t,s)$ is the shear relaxation modulus, ξ is the reduced time, and a_{T} is the shift factor of the time–temperature superposition principle.

For the free or unconstrained quenching, $\sigma \cdot n = 0$.

For constrained quenching, $u = 0$, where n is the unit vector normal to the surface and u is the displacement on the surface.

St-Jacques [87] was the first author to present work on warpage in injection molding flat parts due to unbalanced cooling conditions. He used a one-dimensional, transient heat conduction model (with constant material properties) to predict the temperature profiles in a solidifying slab and used them to estimate the thermal warpage. His simulation, using finite differences, allowed to analyze asymmetrical cooling, and results showed good agreement with experimental data. Nowadays, several approaches have been developed to study the shrinkage, warpage, or residual stresses in injection molded components due to cooling, some of which are summarized in Table 2.

An interesting method for predicting thermal-induced residual stresses in polymeric materials was proposed by Tropsa et al. [99], based on previous work by Williams [100]. They introduced the "residual temperature field" concept to describe the relationship between the thermal history that the material goes through during processing and the frozen-in strains. When this temperature field is applied as an actual temperature distribution, it produces thermal stresses and distortions equal to those caused by residual stresses. The derivation of thermally induced residual stresses starts with the equilibrium equations and the constitutive law for a linear thermoelastic solid. However, the analysis is extended afterward to include anelastic effects to give residual stresses. By knowing the residual temperature field (T_{res}), the residual stress distribution $\sigma_{res}(z)$ can be calculated as

$$\sigma_{res}(z) = \frac{E_\infty}{1 - v}\alpha[\bar{T}_{res} - T_{res}(z)],$$

where E_∞ is the long-term modulus, v is the Poisson ratio, α is the thermal expansion coefficient, and $\bar{T}_{res}$ is the average value of T_{res} through the specimen thickness.

Effective factors of residual stress build-up during injection molding

Several studies have focused on analyzing the effects of different processing parameters, such as mold and melt temperature, packing pressure and time, and injection and cooling rate, on the residual stress distribution on injection molded parts. In most of these studies, warpage has been used as an indicator of residual stresses.

There are two basic approaches on these studies. In one hand, experimental investigations have been carried out, in which processing conditions are varied on each injection cycle, and their effect on residual stresses measured and recorded. Packing pressure, mold and melt temperature, and the design of the cooling system have been pointed out as the most significant processing conditions, with packing pressure as the most important parameter on which shrinkage, warpage, and residual stresses depend, as it can be observed in Table 3 in which results of several authors are summarized. Other processing and design factors such as mold deflection, gate dimensions, and wall thickness have also been studied [101, 102]. However, it has been found that their effect in residual stresses is less significant.

On the other hand, with the development of computational tools, a different software has been used to simulate the flow of the polymer inside the cavities and to predict the part quality after ejection. Again, processing conditions on each simulation are changed and their effect on residual stresses recorded.

Huang and Tai [103] used the experimental design of Taguchi method to determine the effects of injection molding conditions on warpage, and the injection process was simulated using C-MOLD. They found that packing pressure has the greatest effect in warpage, followed by mold temperature, melt temperature, and packing time. However, by analyzing the interaction between factors, they found that the interaction between the mold temperature and melt temperature has in fact a greater effect on warpage than the packing pressure by itself and should not be neglected. Other authors [104–111] have used Taguchi method and injection molding simulation software as Moldflow to minimize warpage and sink marks in injection molded components while obtaining the optimum processing conditions. Gao and Wang [112] proposed a Kriging model in combination with Moldflow simulations to minimize the warpage in injection molding.

More recently, neural networks [113–116] and genetic algorithms [117] have been used to predict the quality of injection molded products and to obtain the optimum processing conditions. Similar to the experimental results, it has been reported that the packing pressure and melt temperature contribute significantly to the shrinkage, warpage, and quality of the injected parts; also, the effect of a higher temperature gradient between polymer melt and mold was overcome by the effect of a higher packing pressure [110, 117].

Although numerical methods combined with statistical tools are useful, some authors [118, 119] suggest that these results should be combined with experimental ones, mainly because factors such as available clamp force, cycle time, and mold surface finish are not considered. Other factors affecting residual stress development are the molecular weight of the polymer (with higher molecular weight polymers resulting in higher residual stresses [120]), its degree of crystallinity [121], its relaxation behavior, and geometric parameters such as thickness and other

Table 2 Thermal-induced stresses models and simulations

Authors	Approach	Results
Thermoelastic models		
Jansen et al. [83, 88–90]	Assumed a simple elastic behavior for the solid. Seneral analytical expressions for stress distributions and shrinkage curves were derived, including effects of pressure, external forces, and crystallization Equations were applied to free quenching and injection molding with hindered shrinkage in the mold	*TCT* distribution before ejection ≈ 10.0/−20.0/6.0 MPa *TCT* distribution after ejection ≈ 4.0/−12.0/12.0 MPa
Denizart et al. [91]	Thermal stresses were estimated assuming an orthotropic thermoelastic behavior for the polymer	Center-gate disks were analyzed. Experimental data was compared with FEM results. Good agreement was found *CT* distribution for PS ≈ −5.0 to −20.0/0.5 to 2.0 MPa depending on processing conditions
Viscoelastic models		
Kabanemi and Crochet [92]	Thermoviscoelastic model considering the cooling stage of injection molding and neglecting the effect of packing pressure	Residual stresses and dimensional changes in injection molded parts in terms of cooling were predicted
Zoetelief et al. [7]	Linear viscoelastic constitutive law to predict thermal stresses Influence of orientation and flow-induced stresses were neglected	In contrast to slabs cooled at ambient pressures which show the well-known tensile stress in the core and compressive in the surfaces, during the packing stage tensile stresses may develop at the surface *TCT* distribution for ABS ≈ 3.0/−7.0/3.0 MPa
Chen et al. [93]	Thermoviscoelastic model, with the initial strain at the beginning of the cooling stage taken as the packing bulk strain	Stresses increase in magnitude moving inwards from the wall. Up to 10.0 MPa in ABS samples
Chang and Tsaur [94]	A control volume method was used to obtain the temperature and pressure profiles Flow- and thermal-induced stresses were obtained with a linear thermoviscoelastic model FEM was used to obtain displacements	Investigated the shrinkage, warpage and sink marks of injection molded parts Experimental results on amorphous ABS plates showed a good correlation with theoretical predictions, which were also correlate using C-MOLD commercial software
Kamal et al. [95]	Linear elastic and linear thermoviscoelastic compressible model applied to thin walls Crystallization effects were considered	Both models provided satisfactory results. However, the thermoviscoelastic analysis provided the best predictions for large stresses developed at the surfaces *TCT* distribution for PS ≈ 0.0/−7.0/5.0 MPa
Liu [96]	Viscoelatic phase transformation model, using a standard linear solid and a viscous fluid model for the solidified polymer and polymer melt, respectively	Simulate and predict thermal residual stresses and warpage *CT* distribution for PS ≈ −7.0/3.0 MPa
Thermorheological models		
Choi and Im [97]	Thermorheological simple viscoelastic material model that uses the temperature and pressure histories developed during the filling and post-filling stages Deformation was analyzed using a linear elastic 3D-finite element approach	Residual stresses were predicted during the packing and cooling stages of injection of amorphous polymers Good agreement with available experimental data in the literature *TCT* distribution for PS ≈ 10.0 to 15.0/−7.0 to −12.0/3.0 to 7.0 MPa
Li and Zhou [98]	Thermorheologically simple viscoelastic material model to consider the stress-relaxation effect in injection molded parts Prediction of warpage using theory of shells	Gate design has an effect on warpage: a fan gate is a little more severe than a rectangular gate All predicted maximum warpages of the part were in agreement with experimental data

TCT tensile-skin/compressive-subskin/tensile-core distribution (Fig. 2c), *CT* compressive-skin/tensile-core distribution (Fig. 2a)

Table 3 Effects of processing conditions on shrinkage, warpage, and residual stresses

Processing parameter	Effect on shrinkage, warpage or residual stresses
Packing pressure	Higher packing pressure: lower shrinkage [24, 119, 123–125]
	Higher packing pressure: lower frozen-in birefringence [42, 43]
	Most significant effect on warpage [103, 105, 111, 126, 127]
	Most significant influence on sink mark depth [110, 117]
	Cavity pressure: indicator of part quality [14, 128]
	Packing pressure effect decreases with fiber content [129]
	Packing pressure affected by mold elastic deformation (overpacking) [101, 102]
Melt temperature	Higher melt temperature: lower residual stresses [1]
	Higher melt temperature: lower shrinkage [124]
	Second significant influence on sink mark depth [110, 117]
Mold temperature	Higher mold temperature: lower residual stresses [1, 130]
	High mold temperature: lower shrinkage [119]
	Higher mold temperature: higher surface tensile stress [36]
	Second important effect on warpage [103, 114]
	Temperature difference between the mold surfaces: main cause of warpage [129, 131]
Injection rate	Lower injection rate: tensile stresses
	Higher flow rate: compressive stresses
	Even higher flow rate: decrease in compressive stresses magnitude [1]
Packing time	Longer holding time: lower shrinkage [83]
	Most significant parameter on shrinkage [126]
Geometry	Thinner gates: more uniform shrinkage [101]
	Gate dimension has only a small influence on warpage [103]
	Triangular rib: most suitable rib for minimizing warpage and sink index [104]
Cooling time	Longer cooling time: lower warpage [111, 118]
	Cooling rate: dominant factor in the development of residual stresses [121, 132–136]

processing considerations such as the use of release agents [122].

Other effects of residual stresses on the performance of injection molded parts

It is well known that residual stresses influence the properties of injection molded products. These stresses act internally at room temperature and have the same effects on the material as externally applied stresses do [122, 137]. Their magnitude can be high enough to induce severe shape changes in the product, as well as changes in the overall material performance.

In addition to the shape distortion, the presence of residual stresses is also expected to affect the mechanical behavior of the product. Broutman et al. [138, 139] found a large increase of the notched Izod impact strength and a decrease in the ductile–brittle transition temperature of PC and other materials when tensile residual stresses were reduced. They suggested that the presence of compressive residual stresses in the surface suppressed craze initiation in advance of the notch [140]. However, in the case of PVC and ABS, the impact properties were not significantly modified by the presence of compressive stresses, leading to the conclusion that the influence of residual stresses on impact strength is only significant on those polymers whose failure initiation is highly localized. When the failure initiation is not limited to a single craze, as in rubber modified polymers, the extent of deformation is controlled by multiple crazing or by shear yielding, and the effect of the compressive residual stresses is limited [138].

Chaoui et al. [141] studied the effect of residual stresses on slow crack propagation in MDPE pipes. They found that the pipes exhibit more resistance to crack propagation in the outer surface than in the inner one, with compressive and tensile residual stresses, respectively. They concluded that the material resistance to fracture is strongly influenced by its thermal history, which determines not only the residual stresses distribution but also the morphology of the material. Guevara and Leevers [142] studied the effect of residual stresses on rapid crack propagation of polyethylene pipes. They found that the lower the residual stress, the lower the S4 (Small Scale Steady State) critical temperature. It was suggested that the additional stored strain energy prior to fracture helps to drive the crack, and that a change in crack front shape due to the release of a bending moment can change crack propagation. Similar results were found by Argyrakis [143]. Davis [144] also found a difference in rapid crack propagation of single and dual cooled pipes; however, he attributed the results mainly to differences in crystallinity.

The effect of residual stresses on the fatigue life of a polymer is also known. Hornberger and Devries [145, 146] found that compressive residual stresses enhance fatigue life, while tensile stresses usually decrease it. Compressive stresses decrease the sensitivity of the polymer to flaws; and since fatigue is dependent on the stress intensity factors at those flaws, the fatigue life is increased. Sauer et al. [147] have reported increases in fatigue life by a factor of 20 in PS with the reduction of tensile stresses. Hornberger and Devries reported a tenfold increase in the mean fatigue life of PC samples [145]; however, they also suggested that the morphology of the polymer also has an important influence on the fatigue life of the polymer.

Siegmann et al. [3] studied the effect of residual stresses on density distribution and tensile properties of quenched PPO specimens. A steep density gradient at the surface of the specimens was found. Tensile modulus and ultimate tensile stress increased significantly from the surface to the inner layers. By analyzing fracture surfaces, they also found that fracture initiation sites and thus the fracture energy are influenced by residual stresses, the latter being higher when fracture initiates at the inner layers.

Turnbull et al. [148] studied the impact of residual stress and molecular orientation on environmental stress cracking. The difference in threshold stress measured for the annealed and as-processed specimens indicated the existence of a net tensile residual stress in the very near-surface region of their specimens.

It has been found that tensile stresses accelerate the rate of photochemical degradation of polymers by accelerating molecular scission, while compressive stresses generally retard it [149–152]. Kwok et al. [153] suggested a premature ejection and quenching of injection molded components with an aim of obtaining compressive stresses at the outer layers and improving resistance against ultraviolet irradiation.

Residual stress measurement techniques

Techniques for characterizing residual stresses in plastics are basically of two types: destructive and non-destructive [5, 154, 155]. Destructive methods are based on the relaxation of strains after the removal of a specific amount of material, and the measurement of these strains to calculate the residual stresses. Non-destructive methods are mainly used to measure stresses at the surface of the specimens, such as photoelastic methods. Hughes et al. [156] also mention predictive techniques, in which computer simulations are used to predict residual stresses; however, results must be validated by experimental data collected using one of the previous techniques.

Destructive methods

Layer removal

The layer-removal technique, first applied to metal sheets, was developed by Treuting and co-author [157]. It involves the removal of successive uniform layers of material from the surface of the specimen and the measurement of the resulting curvatures as a function of specimen thickness. The measured curvature as a function of depth removed can be used to calculate the stress distribution through the thickness of the sample prior to layer removal. The technique has been the primary method used for plastics [158], but the limitation to flat sheets is a major constraint as is the inability to assess very near-surface stresses. In contrast to other methods, it provides a complete picture of the distribution of residual stresses. When the following conditions are satisfied, the accuracy of the method is limited only by the precision of the measurements [157]: the specimen is linear in pure bending for the range of curvature, the stress does not vary in the plane of the specimen but only through the thickness, and the process of removing successive layers does not disturb the stresses in the remaining material.

Coxon and White [159] examined the residual stresses in injection molded PP bars using a stress-relaxation method and the layer-removal technique. The layer-removal technique showed that the stresses near to the surface were compressive and those in the interior tensile. White et al. [160–162] examined the layer-removal technique for determining residual stress distributions for moldings with depth-varying elastic modulus. They concluded that although this is a more exact method, in the majority of cases, the unmodified Treuting and Read procedure is perfectly adequate. Hastenberg et al. [130] used the layer-removal method to determine the influence of annealing on the thermal stress distribution on flat plates of three amorphous polymers: PS, PC, and polyphenylene ether/high-impact polystyrene blend. A good reproductibility was obtained. They found that an annealing treatment significantly reduces the overall stress level, without affecting the stress pattern.

Akay and Ozden [131, 163] measured the residual stresses in injection molded ABS and PC specimen using the layer-removal technique and evaluated the effect of the curvature measurement device on the reliability of the results. The accuracy of the measurements depended on the type of device employed (coordinate machine, dial gage, and optical scanner). A peg/pegboard arrangement was found to enable accurate reproduction of the specimen curvature. As expected, a non-contact method such as an optical scanner produced the most reliable curvature measurements.

As pointed out by Denizart et al. [91], the time elapsed between the layer removal and the measurement of the curvature is critical. Some authors prefer to reduce this time to a minimum [4, 130], while others wait until the curvature reaches its maximum value [1, 164].

Although Siegmann [3] and White [158] consider that machining does not affect the residual stress distribution in a significant way when the correct cutting techniques are used, other authors suggest the opposite [91, 163]. Jansen et al. [165] used an Excimer laser as the milling tool for applying the layer-removal method. They found that some disadvantages associated with the layer-removal method were overcome: stress-relaxation effects were effectively excluded since the heating of adjacent material during milling was shown to be negligible. Moreover, an improvement of the measurement resolution was possible as with the laser technique small layers of well-controlled thickness could be removed.

Hole-drilling

The hole-drilling technique was first proposed by Mathar [166] for residual stress measurement. The technique is relatively simple and has been standardized for metallic plates as ASTM Standard E837 [167]. It is a semi-destructive residual stress measurement technique in which a rosette of strain gages is bonded on the surface of the specimen at the point where residual stresses are to be measured. Then, a hole is drilled precisely through the center, and the measured strains are used to calculate the stresses for the two principal axes in the plane of the sample [168]. Sicot et al. [169] studied the influence of two experimental parameters—the depth of each drilled increment and the influence of the relative position of the strain gages compared with the radius of the hole drilled—on the determination of residual stresses using the incremental hole-drilling method. Results showed that these parameters have a significant effect on the magnitude and stability of the residual stresses, mainly because of significant stresses relaxation. Kim et al. [170] used the incremental hole-drilling method to measure the residual stresses in injection molded PS parts. Results were compared with the ones from the layer-removal method. They found that the measured residual stresses are in fact affected by additional stresses generated during these techniques, and thus the experimental environment needs to be improved. In other work, Kim et al. [171, 172] used the finite element method for calibration of residual stresses in each increment on the hole-drilling method. Residual stress distributions obtained by both experiments and numerical methods accorded well with each other. Maxwell and Turnbull [173] made a comparative evaluation of the layer-removal method and hole-drilling techniques for measurement of residual stress in ABS samples. They found that residual stresses determined by hole drilling were not equi-biaxial and did not balance through the thickness of the specimen, and concluded that although hole-drilling technique is a more flexible technique than layer-removal technique, the results obtained are not as reliable.

Although it is a relatively simple technique, the utilization of the strain gage rosettes presents some practical disadvantages [174] such as the hole must be drilled exactly at the center of the rosette, the strains measured by the gages are average values in the range of the length of the strain gage, and, as in the layer-removal techniques, it is very difficult to identify the additional deformation which resulted from machining (hole drilling). To overcome some of these issues, Chen et al. [174, 175] and Shankar et.al. [176] propose to combine hole-drilling technique with Moiré interferometry, an optical technique that allows to obtain more accurate measurements.

Chemical probe technique

The chemical probe technique is a more speculative approach based on exposing the stressed part or product for a specific period of time to an environment of varying aggressiveness. When a polymer, for example, is immersed in a solvent, it will craze [177–179]. Reference data exist for the relationship between stress and time to crazing for different polymer–environment combinations. Observation of the crazing and the size of the cracks will indicate the level of stresses at the external surface of the part. This technique is also known as solvent crazing, and is similar to the ASTM method for determining residual stresses in ABS parts by immersion in glacial acetic acid [180]. Turnbull et al. [168] used the chemical probe technique to measure the residual stresses in annealed PC and ABS specimens. They concluded that this technique detects only very near tensile surface stresses, which is its major limitation as it lacks the ability to measure the residual stress distribution across the part thickness.

Non-destructive methods

Photoelasticity is a well-known technique for measuring the stress state in complex parts. Residual stresses result in distortion of the polymer chains and induce anisotropy of polarizability, which can be determined by birefringence measurements [168]. Although the technique is limited to transparent materials and its analysis can be complicated due to the effect of molecular orientation induced by processing, it has been successfully applied to the analysis of frozen-in orientation in injection molded samples [40, 181–184]. Wimberger-Friedl and Hendriks [17] measured birefringence in quenched PC specimens. They found that PC is very suitable for the measurement of stress-induced birefringence because of its high positive stress-optical coefficient in the melt and in the glassy state. Wiesauer et al. [185] used polarization-sensitive optical coherence tomography (PS-OCT) to determine and map the internal birefringence properties of PS samples, and obtain information about the stress state within the materials. OCT is an imaging technique capable of recording cross-sectional images of transparent and turbid structures with micrometer-scale resolution [186]. PS-OCT provides additional information on the birefringence properties of a material, as it maps the retardation between the vertical and horizontal polarization components and the orientation of the fast optical axis within the sample, leading to enhanced structural contrast.

Hauk et al. [187] presented an evaluation of different X-ray techniques used to measure residual stresses in semicrystalline polymers. Although some of its limitations are that the specimens should have a crystalline structure and that the measurement depth is limited, and research has extended to amorphous polymers. Barret and Predecki [188, 189] introduced fillers consisting of crystalline particles or powders in amorphous polymers, and then measured their lattice deformation in the injected part by diffracting X-rays at high Bragg angles. Assuming a perfect contact between the particles and the matrix, the stress state was deduced. Hughes et al. [156] used synchrotron X-rays to measure residual strains in commercial HDPE gas pipeline samples. Measurements were feasible in samples of complex geometry and although the technique is used in crystalline polymers, it is suggested that there is also applicability for low- and non-crystalline polymers via the mixing of small volumes of metal powders.

Sanchez and Hornberger [190] used holographic interferometry to monitor the physical relaxation of a plastic-molded component during heating and estimated the initial stress state. Colpo et al. [191] used an embedded Optical Fibre Bragg Grating sensor for characterizing residual strains in an epoxy block during the curing and postcuring stage. Other techniques for measuring residual stresses based on the change in material properties such as refraction of light or electrical conductivity, mainly in thermoplastic composites, are described by Parlevliet et al. [192].

The indentation method, which is almost non-destructive, can be used to measure residual stresses in plastic parts for practical applications, particularly for small or complex parts. Pak et al. [193] applied an indentation method to measure residual stresses in injection molded components. The load–displacement curve was measured for indentation at stressed and non-stressed positions. Residual stress distribution of the injection molded part was calculated by comparing the load–displacement curve results with respect to the indentation depth. Good agreement with numerical results and those measured by the hole-drilling method was found.

Comments on the state of the art

Previous sections show the great effort that has to be done to understand the mechanisms of residual stress build-up. Several models for estimating temperature history during filling, packing, and cooling have been developed, and different models such as the residual temperature field have been applied to estimate thermal residual stresses. The same has happened for flow-induced stress, although more complex situations have been found here. The viscoelastic nature of polymers and the high shear and pressure conditions to which the polymer is subjected to, result in a complex flow of the polymer inside the mold, which in turns results in a complex deformation, orientation, stretching, and relaxation of polymer chains. All these set up residual stresses, which results in part warpage and shrinkage.

Most of these models assume constant through thickness polymer properties, such as constant modulus, density, thermal properties, and orientation, among others, which is far from reality. A more detailed analysis is needed for more complex shapes where the thickness varies across the geometry, and where processing conditions generate different temperature and pressure histories, and thus different polymer structures and properties, affecting the residual stress distribution.

Despite the huge effort for estimating warpage, most of the work has focused on simple geometries such as flat plates, disks, L-shaped specimens, and rectangular boxes. Estimation of warpage of more complex parts is challenging as the polymer melt faces different restrictions during flow which changes the polymer chains' orientation. During filling and packing, restriction comes from the mold itself, while after ejection, it is the part geometry which inhibits uniform shrinkage and polymer chains relaxation. Although some authors have worked with ribbed specimens [84], other common features such as snap fits and bosses require attention, especially in parts subjected to critical loading.

Another interesting area to pursuit is simulation. Commercial software predict warpage of injection molded components based on semi-empirical data. Developing a model that can cope with complex geometries and be used on finite element analysis is needed. As mentioned previously, simulations must be accompanied by experimental data and one way to achieve it is using instrumented molds for complex geometries, in which pressure and temperature histories could be monitored and a detailed analysis of the effect of different processing conditions in residual stress built up could be done.

Finally, transformation-induced residual stresses might need special attention. Although some models consider crystallization and include its effect on changing density, modulus and other properties, the effect of spherulite formation on the volume of the part might be of interest.

References

1. Siegmann A, Buchman A, Kenig S (1982) Residual stresses in polymers III: The influence of injection-molding process conditions. Polym Eng Sci 22:560–568
2. Siegmann A, Buchman A, Kenig S (1982) Residual stresses in polymers I: the effect of thermal history. Polym Eng Sci 22:40–47
3. Siegmann A, Buchman A, Kenig S (1981) Residual stresses in polymers. II. Their effect on mechanical behavior. Polym Eng Sci 21:997–1002
4. Isayev AI, Crouthamel DL (1984) Residual stress development in the injection molding of polymers. Polym Plast Technol 22:177–232
5. Daly HB, Nguyen K, Sanschagrin B, Cole K (1998) Build-up and measurement of molecular orientation, crystalline morphology, and residual stresses in injection molded parts: a review. J Inject Molding Technol 2:59–85
6. Baaijens FPT (1991) Calculation of residual stresses in injection molded products. Rheol Acta 30:284–299
7. Zoetelief WF, Douven LFA, Ingen Housz AJ (1996) Residual thermal stresses in injection molded products. Polym Eng Sci 36:1886–1896
8. Young W-B (2004) Residual stress induced by solidification of thermoviscoelastic melts in the postfilling stage. J Mater Process Technol 145:317–324
9. Shia-Chung C, Yung-Cheng C (1994) Calculations of the flow-induced residual stress development in the injection moulded plate. Comput Struct 52:1043–1050
10. Jansen K (1998) Measurement and prediction of anisotropy in injection moulded PP products. Int Polym Process 13:309–317
11. Wimberger-Friedl R (1995) The assessment of orientation, stress and density distributions in injection-molded amorphous polymers by optical techniques. Prog Polym Sci 20:369–401
12. Sjönell Y, Terselius B, Jansson J-F (1995) Injection molding of polypropylene discs. I: Effect of holding pressure on orientation distribution. Polym Eng Sci 35:950–956
13. Chiang HH, Hieber CA, Wang KK (1991) A unified simulation of the filling and postfilling stages in injection molding. Part II: Experimental verification. Polym Eng Sci 31:125–139
14. Kazmer D, Barkan P (1997) Multi-cavity pressure control in the filling and packing stages of the injection molding process. Polym Eng Sci 37:1865–1879
15. Siegmann A, Kenig S, Buchman A (1987) Residual stresses in injection-molded amorphous polymers. Polym Eng Sci 27:1069–1078
16. Douven LFA, Baaijens FPT, Meijer HEH (1995) The computation of properties of injection-moulded products. Prog Polym Sci 20:403–457
17. Wimberger-Friedl R, Hendriks RDHM (1989) The measurement and calculation of birefringence in quenched polycarbonate specimens. Polymer 30:1143–1149
18. Zhou H, Li D (2005) Residual stress analysis of the post-filling stage in injection moulding. Int J Adv Manuf Technol 25:700–704
19. Kim KH, Isayev AI, Kwon K, van Sweden C (2005) Modeling and experimental study of birefringence in injection molding of semicrystalline polymers. Polymer 46:4183–4203
20. Isayev AI, Shyu GD, Li CT (2006) Residual stresses and birefringence in injection molding of amorphous polymers: simulation and comparison with experiment. J Polym Sci Pol Phys 44:622–639
21. Lee YB, Kwon TH (2001) Modeling and numerical simulation of residual stresses and birefringence in injection molded center-gated disks. J Mater Process Technol 111:214–218
22. Janeschitz-Kriegl H (1977) Injection moulding of plastics: some ideas about the relationship between mould filling and birefringence. Rheol Acta 16:327–339
23. Cao W, Shen C, Zhang C, Wang L (2008) Computing flow-induced stresses of injection molding based on the Phan–Thien–Tanner model. Arch Appl Mech 78:363–377
24. Bushko WC, Stokes VK (1995) Solidification of thermoviscoelastic melts. Part II: Effects of processing conditions on shrinkage and residual stresses. Polym Eng Sci 35:365–383
25. Bushko WC, Stokes VK (1996) Solidification of thermoviscoelastic melts. Part 3: Effects of mold surface temperature differences on warpage and residual stresses. Polym Eng Sci 36:322–335
26. Bushko WC, Stokes VK (1996) Solidification of thermoviscoelastic melts. Part 4: Effects of boundary conditions on shrinkage and residual stresses. Polym Eng Sci 36:658–675
27. Bushko WC, Stokes VK (1995) Solidification of thermoviscoelastic melts. Part I: Formulation of model problem. Polym Eng Sci 35:351–364
28. Zhang N, Gilchrist MD (2012) Characterization of thermo-rheological behavior of polymer melts during the micro injection moulding process. Polym Test 31:748–758
29. Baltussen MGHM, Hulsen MA, Peters GWM (2010) Numerical simulation of the fountain flow instability in injection molding. J Non Newton Fluid 165:631–640
30. Yang B, Ouyang J, Liu C, Li Q (2010) Simulation of non-isothermal injection molding for a non-Newtonian fluid by level set method. Chin J Chem Eng 18:600–608
31. Tanner RI (2003) On the flow of crystallizing polymers: I. Linear regime. J Non Newton Fluid 112:251–268
32. Vinogradov V (1975) Residual stresses in plastic parts. Plast Massy 4:20–31
33. Jansen K (1994) Residual stresses in quenched and injection moulded products. Int Polym Proc 9:82–89
34. Sandilands GJ, White JR (1980) Effect of injection pressure and crazing on internal stresses in injection-moulded polystyrene. Polymer 21:338–343
35. Mlekusch B (2001) Calculation of residual stress development in injection moulding using a nonlinear viscoelastic model. Mech Time Depend Mater 5:101–118
36. Wang T-H, Young W-B (2005) Study on residual stresses of thin-walled injection molding. Eur Polym J 41:2511–2517
37. Jansen K, Van Dijk DJ, Keizer KP (1998) Warpage of injection moulded plates and corner products. Int Polym Proc 13:417–424
38. Leonov AI (1976) Nonequilibrium thermodynamics and rheology of viscoelastic polymer media. Rheol Acta 15:85–98
39. Kabanemi KK, Aït-Kadi A, Tanguy P (1995) Prediction of residual flow and thermoviscoelastic stresses in injection molding. Rheol Acta 34:97–108

40. Isayev AI, Hieber CA (1980) Toward a viscoelastic modelling of the injection molding of polymers. Rheol Acta 19:168–182
41. Mavridis H, Hrymak AN, Vlachopoulos J (1988) The effect of fountain flow on molecular orientation in injection molding. J Rheol 32:639–663
42. Flaman AAM (1993) Buildup and relaxation of molecular orientation in injection molding. Part II: Experimental verification. Polym Eng Sci 33:202–210
43. Flaman AAM (1993) Buildup and relaxation of molecular orientation in injection molding. Part I: Formulation. Polym Eng Sci 33:193–201
44. Spencer R, Gilmore G (1950) Equation of state for high polymers. J Appl Phys 21:523–526
45. Greener J, Kesel R, Contestable BA (1989) The birefringence problem in optical disk substrates: a modeling approach. AlChE J 35:449–458
46. Wagner MH (1976) Analysis of stress-growth data for simple extension of a low-density branched polyethylene melt. Rheol Acta 15:133–135
47. Matsui M, Bogue D (1977) Studies in non-isothermal rheology. J Rheol 21:133
48. Xue SC, Phan-Thien N, Tanner RI (1998) Three dimensional numerical simulations of viscoelastic flows through planar contractions. J Non Newton Fluid 74:195–245
49. Marchal JM, Crochet MJ (1987) A new mixed finite element for calculating viscoelastic flow. J Non Newton Fluid 26:77–114
50. Zhou H, Xi G, Liu F (2008) Residual stress simulation of injection molding. J Mater Eng Perform 17:422–427
51. Yu F, Zhang H, Zheng H, Yu W, Zhou C (2008) Experimental study of flow-induced crystallization in the blends of isotactic polypropylene and poly(ethylene-co-octene). Eur Polym J 44:79–86
52. Keum JK, Mao Y, Zuo F, Hsiao BS (2013) Flow-induced crystallization precursor structure in high molecular weight isotactic polypropylene (HMW-iPP)/low molecular weight linear low density polyethylene (LMW-LLDPE) binary blends. Polymer 54:1425–1431
53. Janeschitz-Kriegl H, Ratajski E (2005) Kinetics of polymer crystallization under processing conditions: transformation of dormant nuclei by the action of flow. Polymer 46:3856–3870
54. Mu Y, Zhao G, Chen A, Wu X (2012) Numerical investigation of the thermally and flow induced crystallization behavior of semi-crystalline polymers by using finite element–finite difference method. Comput Chem Eng 46:190–204
55. Hsiung CM, Cakmak M, Ulcer Y (1996) A structure oriented model to simulate the shear induced crystallization in injection moulded polymers: a Lagrangian approach. Polymer 37:4555–4571
56. Nielsen LE (1954) Effect of crystallinity on the dynamic mechanical properties of polyethylenes. J Appl Phys 25:1209–1212
57. Brady DG (1976) The crystallinity of poly(phenylene sulfide) and its effect on polymer properties. J Appl Polym Sci 20:2541–2551
58. Starkweather HW, Moore GE, Hansen JE, Roder TM, Brooks RE (1956) Effect of crystallinity on the properties of nylons. J Polym Sci 21:189–204
59. Richards RB (1951) Polyethylene-structure, crystallinity and properties. J Appl Chem 1:370–376
60. Nagamatsu K, Takemura T, Yoshitomi T, Takemoto T (1958) Effect of crystallinity on the viscoelastic properties of polyethylene. J Polym Sci 33:515–518
61. Wright DGM, Dunk R, Bouvart D, Autran M (1988) The effect of crystallinity on the properties of injection moulded polypropylene and polyacetal. Polymer 29:793–796
62. Santis FD, Pantani R, Speranza V, Titomanlio G (2010) Analysis of shrinkage development of a semicrystalline polymer during injection molding. Ind Eng Chem Res 49:2469–2476
63. Pantani R, Coccorullo I, Speranza V, Titomanlio G (2007) Morphology evolution during injection molding: effect of packing pressure. Polymer 48:2778–2790
64. Zhang X, Li Z, Lu Z, Sun CC (2002) The crystallization of low-density polyethylene: a molecular dynamics simulation. Polymer 43:3223–3227
65. Xu JT, Wang Q, Fan ZQ (2005) Non-isothermal crystallization kinetics of exfoliated and intercalated polyethylene/montmorillonite nanocomposites prepared by in situ polymerization. Eur Polym J 41:3011–3017
66. Wagner J, Phillips PJ (2001) The mechanism of crystallization of linear polyethylene, and its copolymers with octene, over a wide range of supercoolings. Polymer 42:8999–9013
67. Mubarak Y, Harkin-Jones EMA, Martin PJ, Ahmad M (2001) Modeling of non-isothermal crystallization kinetics of isotactic polypropylene. Polymer 42:3171–3182
68. Lim BA, McGuire KS, Lloyd DR (1993) Non-isothermal crystallization of isotactic polypropylene in dotriacontane. II: Effects of dilution, cooling rate, and nucleating agent addition on growth rate. Polym Eng Sci 33:537–542
69. Brucato V, Crippa G, Piccarolo S, Titomanlio G (1991) Crystallization of polymer melts under fast cooling. I: Nucleated polyamide. Polym Eng Sci 6(31):1411–1416
70. Di Lorenzo ML, Silvestre C (1999) Non-isothermal crystallization of polymers. Prog Polym Sci 24:917–950
71. Jiao C, Wang Z, Liang X, Hu Y (2005) Non-isothermal crystallization kinetics of silane crosslinked polyethylene. Polym Test 24:71–80
72. Nakamura K, Katayama K, Amano T (1973) Some aspects of nonisothermal crystallization of polymers. II. Consideration of the isokinetic condition. J Appl Polym Sci 17:1031–1041
73. Phillips R, Manson JE (1997) Prediction and analysis of nonisothermal crystallization of polymers. J Polym Sci B 35:875–888
74. Pantani R, Coccorullo I, Speranza V, Titomanlio G (2005) Modeling of morphology evolution in the injection molding process of thermoplastic polymers. Prog Polym Sci 30:1185–1222
75. Gardon R, Narayanaswamy OS (1970) Stress and volume relaxation in annealing flat glass. J Am Ceram Soc 53:380–385
76. Lee EH, Rogers TG, Woo TC (1965) Residual stresses in a glass plate cooled symmetrically from both surfaces. J Am Ceram Soc 48:480–487
77. Aggarwala B, Saibel E (1961) Tempering stresses in an infinite glass plate. Phys Chem Glasses 2:137–140
78. Narayanaswamy OS, Gardon R (1969) Calculation of residual stresses in glass. J Am Ceram Soc 52:554–558
79. Mauch F, Jäckle J (1994) Thermoviscoelastic theory of freezing of stress and strain in a symmetrically cooled infinite glass plate. J Non Cryst Solids 170:73–86
80. Adams LH, Williamson ED (1920) The annealing of glass. J Franklin I 190:835–870
81. Struik LCE (1978) Orientation effects and cooling stresses in amorphous polymers. Polym Eng Sci 18:799–811
82. Rigdahl M (1976) Calculation of residual thermal stresses in injection molded amorphous polymers by the finite element method. Int J Polym Mater 5:43–57
83. Jansen K, Titomanlio G (1996) Effect of pressure history on shrinkage and residual stresses—injection molding with constrained shrinkage. Polym Eng Sci 36:2029–2040
84. Zheng R, Kennedy P, Phan-Thien N, Fan XJ (1999) Thermoviscoelastic simulation of thermally and pressure-induced stresses in injection moulding for the prediction of shrinkage and warpage for fibre-reinforced thermoplastics. J Non Newton Fluid 84:159–190
85. Kwon Y, Kang T, Chung K, Youn J (2001) Prediction and measurement of residual stresses in injection molded parts. Fibers Polym 2:203–211

86. Wu H, Zhao Z, Sha J (2009) Experiments and prediction of in-cavity stress for injection molded part. Mech Time Depend Mater 13:233–244
87. Jacques MS (1982) An analysis of thermal warpage in injection molded flat parts due to unbalanced cooling. Polym Eng Sci 22:241–247
88. Jansen KMB, Van Dijk DJ, Freriksen MJA (1998) Shrinkage anisotropy in fiber reinforced injection molded products. Polym Compos 19:325–334
89. Jansen KMB, Pantani R, Titomanlio G (1998) As-molded shrinkage measurements on polystyrene injection molded products. Polym Eng Sci 38:254–264
90. Titomanlio G, Jansen KMB (1996) In-mold shrinkage and stress prediction in injection molding. Polym Eng Sci 36:2041–2049
91. Denizart O, Vincent M, Agassant JF (1995) Thermal stresses and strains in injection moulding: experiments and computations. J Mater Sci 30:552–560. doi:10.1007/BF00354424
92. Kabanemi KK, Crochet MJ (1992) Thermoviscoelastic calculation of residual stresses and residual shapes of injection molded parts. Int Polym Proc 1:60–70
93. Chen X, Lam YC, Li DQ (2000) Analysis of thermal residual stress in plastic injection molding. J Mater Process Technol 101:275–280
94. Chang RY, Tsaur BD (1995) Experimental and theoretical studies of shrinkage, warpage, and sink marks of crystalline polymer injection molded parts. Polym Eng Sci 35:1222–1230
95. Kamal MR, Lai-Fook RA, Hernandez-Aguilar JR (2002) Residual thermal stresses in injection moldings of thermoplastics: a theoretical and experimental study. Polym Eng Sci 42:1098–1114
96. Liu S-J (1996) Modeling and simulation of thermally induced stress and warpage in injection molded thermoplastics. Polym Eng Sci 36:807–818
97. Choi D-S, Im Y-T (1999) Prediction of shrinkage and warpage in consideration of residual stress in integrated simulation of injection molding. Compos Struct 47:655–665
98. Li D, Zhou H (2004) Modelling and simulation of residual stress and warpage in injection moulding. Proc Inst Mech Eng C 218:521–530
99. Tropsa V, Ivankovic A, Williams JG (2000) Predicting residual stresses due to solidification in cast plastic plates. Plast Rub Compos 29:468–474
100. Williams JG (1981) On the prediction of residual stresses in polymers. Plast Rub Proc Appl 1:369–377
101. Leo V, Cuvelliez C (1996) The effect of the packing parameters, gate geometry, and mold elasticity on the final dimensions of a molded part. Polym Eng Sci 36:1961–1971
102. Delaunay D, Le Bot P, Fulchiron R, Luye JF, Regnier G (2000) Nature of contact between polymer and mold in injection molding. Part II: Influence of mold deflection on pressure history and shrinkage. Polym Eng Sci 40:1692–1700
103. Huang M-C, Tai C-C (2001) The effective factors in the warpage problem of an injection-molded part with a thin shell feature. J Mater Process Technol 110:1–9
104. Erzurumlu T, Ozcelik B (2006) Minimization of warpage and sink index in injection-molded thermoplastic parts using Taguchi optimization method. Mater Design 27:853–861
105. Ozcelik B, Sonat I (2009) Warpage and structural analysis of thin shell plastic in the plastic injection molding. Mater Design 30:367–375
106. Song MC, Liu Z, Wang MJ, Yu TM, Zhao DY (2007) Research on effects of injection process parameters on the molding process for ultra-thin wall plastic parts. J Mater Process Technol 187–188:668–671
107. Öktem H (2012) Modeling and analysis of process parameters for evaluating shrinkage problems during plastic injection molding of a DVD-ROM cover. J Mater Eng Perform 21:25–32
108. Chen C-C, Su P-L, Lin Y-C (2009) Analysis and modeling of effective parameters for dimension shrinkage variation of injection molded part with thin shell feature using response surface methodology. Int J Adv Manuf Technol 45:1087–1095
109. Chiang K-T, Chang F-P (2006) Analysis of shrinkage and warpage in an injection-molded part with a thin shell feature using the response surface methodology. Int J Adv Manuf Technol 35:468–479
110. Mathivanan D, Parthasarathy NS (2009) Prediction of sink depths using nonlinear modeling of injection molding variables. Int J Adv Manuf Technol 43:654–663
111. Wang X, Zhao G, Wang G (2013) Research on the reduction of sink mark and warpage of the moulded part in rapid heat cycle moulding process. Mater Design 47:779–792
112. Gao Y, Wang X (2008) An effective warpage optimization method in injection molding based on the Kriging model. Int J Adv Manuf Technol 37:953–960
113. Lotti C, Ueki MM, Bretas RES (2002) Prediction of the shrinkage of injection molded iPP plaques using artificial neural networks. J Inject Molding Technol 6:157–176
114. Chen W-C, Tai P-H, Wang M-W, Deng W-J, Chen C-T (2008) A neural network-based approach for dynamic quality prediction in a plastic injection molding process. Expert Syst Appl 35:843–849
115. Shie J-R (2008) Optimization of injection molding process for contour distortions of polypropylene composite components by a radial basis neural network. Int J Adv Manuf Technol 36:1091–1103
116. Altan M (2010) Reducing shrinkage in injection moldings via the Taguchi, ANOVA and neural network methods. Mater Design 31:599–604
117. Mathivanan D, Parthasarathy NS (2009) Sink-mark minimization in injection molding through response surface regression modeling and genetic algorithm. Int J Adv Manuf Technol 45:867–874
118. Sánchez R, Aisa J, Martinez A, Mercado D (2012) On the relationship between cooling setup and warpage in injection molding. Measurement 45:1051–1056
119. Kurt M, Saban Kamber O, Kaynak Y, Atakok G, Girit O (2009) Experimental investigation of plastic injection molding: assessment of the effects of cavity pressure and mold temperature on the quality of the final products. Mater Design 30:3217–3224
120. Kazakov A (1998) An automated method for the measurement of residual stress in melt-extruded plastic pipes. Polym Test 17:443–450
121. Glomsaker T, Larsen A, Andreassen E (2005) Experimental and numerical investigation of warpage of semicrystalline polymers in rotational molding. Polym Eng Sci 45:945–952
122. Xu H, Bellehumeur CT (2008) Thermal residual stress development for semi-crystalline polymers in rotational molding. Polym Eng Sci 48:283–291
123. Postawa P, Koszkul J (2005) Change in injection moulded parts shrinkage and weight as a function of processing conditions. J Mater Process Technol 162–163:109–115
124. Jansen KMB, Van Dijk DJ, Husselman MH (1998) Effect of processing conditions on shrinkage in injection molding. Polym Eng Sci 38:838–846
125. Aisa J, Castany J (2009) Dimensional study of thermoplastic parts made using sequential injection molding. Polym Eng Sci 49:1832–1838
126. Oktem H, Erzurumlu T, Uzman I (2007) Application of Taguchi optimization technique in determining plastic injection molding process parameters for a thin-shell part. Mater Design 28:1271–1278
127. Chen C-P, Chuang M-T, Hsiao Y-H, Yang Y-K, Tsai C-H (2009) Simulation and experimental study in determining injection

molding process parameters for thin-shell plastic parts via design of experiments analysis. Expert Syst Appl 36:10752–10759
128. Angstadt DC, Coulter JP (1999) Cavity pressure and part quality in the injection molding process. Intell Mater Manuf Lab Lehigh Univ, Pennsylvania
129. Kovács JG, Sikló B (2011) Test method development for deformation analysis of injection moulded plastic parts. Polym Test 30:543–547
130. Hastenberg CHV, Wildervanck PC, Leenen AJH, Schennink GGJ (1992) The measurement of thermal stress distributions along the flow path in injection-molded flat plates. Polym Eng Sci 32:506–515
131. Akay M, Ozden S, Tansey T (1996) Prediction of process-induced warpage in injection molded thermoplastics. Polym Eng Sci 36:1839–1846
132. Clutton EQ, Williams JG (1995) On the measurement of residual stress in plastic pipes. Polym Eng Sci 35:1381–1386
133. Hassan H, Regnier N, Le Bot C, Defaye G (2010) 3D study of cooling system effect on the heat transfer during polymer injection molding. Int J Therm Sci 49:161–169
134. Hassan H, Regnier N, Pujos C, Arquis E, Defaye G (2010) Modeling the effect of cooling system on the shrinkage and temperature of the polymer by injection molding. Appl Therm Eng 30:1547–1557
135. Tang LQ, Chassapis C, Manoochehri S (1997) Optimal cooling system design for multi-cavity injection molding. Finite Elem Anal Des 26:229–251
136. Qiao H (2006) A systematic computer-aided approach to cooling system optimal design in plastic injection molding. Int J Mech Sci 48:430–439
137. Mills NJ (1982) Residual stresses in plastics, rapidly cooled from the melt, and their relief by sectioning. J Mater Sci 17:558–574. doi:10.1007/BF00591490
138. Thakkar BS, Broutman LJ (1980) The influence of residual stresses and orientation on the properties of amorphous polymers. Polym Eng Sci 20:1214–1219
139. Broutman LJ, Krishnakumar SM (1976) Impact strength of polymers: 1. The effect of thermal treatment and residual stress. Polym Eng Sci 16:74–81
140. So P, Broutman LJ (1976) Residual stresses in polymers and their effect on mechanical behavior. Polym Eng Sci 16:785–791
141. Chaoui K, Chudnovsky A, Moet A (1987) Effect of residual stress on crack propagation in MDPE pipes. J Mater Sci 22:3873–3879. doi:10.1007/BF01133334
142. Guevara-Morales A, Leevers P (2013) Experimental investigation of the effect of residual stresses on rapid crack propagation in polyethylene (PE100) pipes. Polym Eng Sci 53:1217–1222
143. Argyrakis C (2010) Department of Mechanical Engineering, Imperial College London, London, UK
144. Davis P (1999) Mechanical Engineering Department, Imperial College London, London, UK
145. Hornberger LE, Devries KL (1987) The effect of residual stress on the mechanical properties of glassy polymers. Polym Eng Sci 27:1473–1478
146. Hornberger LE, DeVries KL (1987) Measurement of favorable residual stresses in polycarbonate. Exp Mech 27:94–98
147. Sauer JA, Habibullah M, Chen CC (1981) Fatigue of high impact polystyrene and influence of surface treatments. J Appl Phys 52:5970–5976
148. Turnbull A, Maxwell AS, Pillai S (2000) Comparative assessment of slow strain rate, 4-pt bend and constant load test methods for measuring environment stress cracking of polymers. Polym Test 19:117–129
149. O'Donnell B, White JR (1994) Stress-accelerated photo-oxidation of polypropylene and glass–fibre-reinforced polypropylene. Polym Degrad Stab 44:211–222
150. Shyichuk AV, White JR (2000) Analysis of chain-scission and crosslinking rates in the photo-oxidation of polystyrene. J Appl Polym Sci 77:3015–3023
151. Tyler DR (2004) Mechanistic aspects of the effects of stress on the rates of photochemical degradation reactions in polymers. J Macromol Sci 44:351–388
152. Chen R, Tyler DR (2004) Origin of tensile stress-induced rate increases in the photochemical degradation of polymers. Macromolecules 37:5430–5436
153. Kwok CS, Tong L, White JR (1996) Generation of large residual stresses in injection moldings. Polym Eng Sci 36:651–657
154. Withers PJ, Bhadeshia HKDH (2001) Residual stress Part 1—measurement techniques. Mater Sci Technol 17:355–365
155. Ruud CO (1982) A review of selected non-destructive methods for residual stress measurement. NDT Int 15:15–23
156. Hughes DJ, Heeley EL, Curfs C (2011) A non-destructive method for the measurement of residual strains in semi-crystalline polymer components. Mater Lett 65:530–533
157. Treuting RG, Read J WT (1951) A mechanical determination of biaxial residual stress in sheet materials. J Appl Phys 22:130–134
158. White JR (1984) Origins and measurements of internal stress in plastics. Polym Test 4:165–191
159. Coxon LD, White JR (1980) Residual stresses and aging in injection molded polypropylene. Polym Eng Sci 20:230–236
160. White JR (1985) On the layer removal analysis of residual stress. J Mater Sci 20:2377–2387. doi:10.1007/BF00556067
161. Paterson MWA, White JR (1989) Layer removal analysis of residual stress. J Mater Sci 24:3521–3528. doi:10.1007/BF02385734
162. Haworth B, Hindle C, Sandilands G, White J (1982) Assessment of internal stresses in injection-molded thermoplastics. Plast Rub Proc Appl 2:59–71
163. Akay M, Ozden S (1994) Measurement of residual stresses in injection moulded thermoplastics. Polym Test 13:323–354
164. Pham HT, Bosnyak CP, Sehanobish K (1993) Residual stresses in injection molded polycarbonate rectangular bars. Polym Eng Sci 33:1634–1643
165. Jansen KMB, Orij JJW, Meijer CZ, Dijk DJV (1999) Comparison of residual stress predictions and measurements using excimer laser layer removal. Polym Eng Sci 39:2030–2041
166. Mathar J (1934) Determination of initial stresses by measuring the deformation around drilled holes. Trans ASME 56:249–254
167. ASTM E837-08 (2009) Standard test method for determining residual stresses by the hole-drilling strain-gage method, p 17
168. Turnbull A, Maxwell AS, Pillai S (1999) Residual stress in polymers—evaluation of measurement techniques. J Mater Sci 34:451–459. doi:10.1023/A:1004574024319
169. Sicot O, Gong XL, Cherouat A, Lu J (2004) Influence of experimental parameters on determination of residual stress using the incremental hole-drilling method. Compos Sci Technol 64:171–180
170. Kim C, Kim S, Oh H, Youn J (2007) Measurement of residual stresses in injection molded polymeric part by applying layer-removal and incremental hole-drilling methods. Fibers Polym 8:443–446
171. Kim CH, Youn JR (2007) Determination of residual stresses in injection-moulded flat plate: simulation and experiments. Polym Test 26:862–868
172. Kim SY, Kim CH, Kim SH, Oh HJ, Youn JR (2009) Measurement of residual stresses in film insert molded parts with complex geometry. Polym Test 28:500–507
173. Maxwell AS, Turnbull A (2003) Measurement of residual stress in engineering plastics using the hole-drilling technique. Polym Test 22:231–233
174. Chen J, Peng Y, Zhao S (2009) Comparison between grating rosette and strain gage rosette in hole-drilling combined systems. Opt Laser Eng 47:935–940

175. Chen J, Peng Y, Zhao S (2009) Hole-drilling method using grating rosette and Moiré interferometry. Acta Mech Sin 25:389–394
176. Shankar K, Xie H, Wei R, Asundi A, Boay CG (2004) A study on residual stresses in polymer composites using moiré interferometry. Adv Compos Mater 13:237–253
177. Cornélis H, Kander RG, Martin JP (1996) Solvent-induced crystallization of amorphous poly(ether ether ketone) by acetone. Polymer 37:4573–4578
178. Clay SB, Kander RG (2001) A new method to quantify crazing in various environments. Polym Eng Sci 41:401–407
179. Cornélis H, Kander RG (1996) A new method to evaluate solvent stress cracking. Polym Eng Sci 36:869–878
180. ASTM D1939-94 (1994) Practice for determining residual stresses in extruded or molded acrylonitrile-butadiene-styrene (ABS) parts by immersion in glacial acetic acid (withdrawn 1999)
181. Wales JLS, Van Leeuwen IJ, Van Der Vijgh R (1972) Some aspects of orientation in injection molded objects. Polym Eng Sci 12:358–363
182. Isayev AI (1983) Orientation development in the injection molding of amorphous polymers. Polym Eng Sci 23:271–284
183. Fernandez-Ballester L, Gough T, Meneau F et al (2008) Simultaneous birefringence, small- and wide-angle X-ray scattering to detect precursors and characterize morphology development during flow-induced crystallization of polymers. J Synchroton Radiat 15:185–190
184. Saffell JR, Windle AH (1980) The influence of thermal history on internal stress distributions in sheets of PMMA and polycarbonate. J Appl Polym Sci 25:1117–1129
185. Wiesauer K, Dufau ADS, Götzinger E, Pircher M, Hitzenberger CK, Stifter D (2005) Non-destructive quantification of internal stress in polymer materials by polarisation sensitive optical coherence tomography. Acta Mater 53:2785–2791
186. Stifter D, Burgholzer P, Höglinger O, Götzinger E, Hitzenberger CK (2003) Polarisation-sensitive optical coherence tomography for material characterisation and strain-field mapping. Appl Phys A 76:947–951
187. Hauk V, Troost A, Ley D (1987) Evaluation of (residual) stresses in semicrystalline polymers by X-rays. Adv Polym Technol 7:389–396
188. Barrett CS, Predecki P (1976) Stress measurement in polymeric materials by X-ray diffraction. Polym Eng Sci 16:602–608
189. Barrett CS, Predecki P (1980) In: Rhodes J, Barret C, Leyden D, Newkirk J, Predecki P, Ruud C (eds) Advances in X-ray analysis. Springer, New York
190. Sanchez LA, Hornberger LE (2002) Monitoring of residual stresses in injection-molded plastics with holographic interferometry. Opt Laser Eng 37:27–37
191. Colpo F, Humbert L, Giaccari P, Botsis J (2006) Characterization of residual strains in an epoxy block using an embedded FBG sensor and the OLCR technique. Composites A 37:652–661
192. Parlevliet PP, Bersee HEN, Beukers A (2007) Residual stresses in thermoplastic composites—a study of the literature—Part II: Experimental techniques. Composites A 38:651–665
193. Pak SY, Kim SY, Kim SH, Youn JR (2013) Measurement of residual stresses in polymeric parts by indentation method. Polym Test 32:946–952